Study Effect of chimney height on the power output of the Solar Chimney System

Rabia AL. Galia [*]

Faculty of Natural Resources- Al. Ajaylat, University of Zawia, Libya

Abstract

For the performance evaluation of a solar chimney power plant (SCPP) with and without heat storage, a full theoretical model has been developed, which has been verified by experimental data from the Spanish prototype and experimental data from a small solar chimney pilot. The experiment was performed at the Sabratha College of Engineering. This model takes into account the effects of heat flux and heat loss, as well as the rates of temperature drop inside and outside the chimney. There was good agreement between these results and those of

(∗) Email: rabee3386@gmail.com

the mathematical model. Hence, the model can be used to analyze solar chimney systems. In this paper, the effect of the chimney height by convection, which avoids negative buoyancy in the latter chimney, and the optimal height of the chimney for maximum performance are presented and analyzed. Under unloaded conditions, it has been reported that the theoretical power output of an SCPP is directly proportional to the height of the chimney. and the output power increases as the chimney height increases, but the rate of increase should be compared to the cost of building a very high chimney.

Keywords: *Solar chimney; buoyancy effect; chimney height; renewable energy.*

1 Introduction

Solar chimney power plant (SCPP) is a relatively novel technology for electricity production from solar energy. The SCPP consists of a greenhouse roof collector and updraft chimney that is located at the centre of the greenhouse roof collector. The greenhouse roof collector is usually made of a plastic sheet or glass plate which traps solar energy. No full-scale solar chimney power plant has been operated to date; however, many proposals have been investigated in different parts of the world. The feasibility of SCPP was evaluated by different experimental studies. a real implementation of Solar Chimney Power Plant SCPP was implemented in 1982 in Manzanares, Spain [1]. Its peak output of power was about 50 kW. In order to evaluate the solar chimney model, a prototype was constructed in Alain, United Arab Emirates (UAE) [2]. The study reported the effect of internal collector dynamic temperature, the amount of solar energy trapped within the collector. In 2018 two similar experimental models were built to achieve the performance of

these new design was conducted by Ahmed, O. K., & Hussein, A. S. [3]. System (A) had a collector glass roof cover and a PV panel as an absorber with a chimney of 2 m height while system (B) is similar to the system (A) but with PV panel as collector roof cover and plywood as an absorber in the base of the chimney. Practical tests were conducted in Kirkuk (35° 28' latitude and 44° 24' longitude), northern Iraq. The results showed that system (A) had higher thermal gain than system B while the daily average of electrical power in the system (B) was (75.6 W) higher than system (A) (79 W). This is because the high thermal gain raised the operating temperature of the PV panel which led to a decrease in its power output. The results also presented that system (A) converted thermal power to kinetic power with a daily average (0.008 W) because of the great thermal gain which made air less dense in turn increased its velocity more than system (B) (0.006 W) which had lower kinetic power. The total useful power produced by the system (B) is greater than the useful power produced from the system (A). Several theoretical studies of solar chimney systems were developed by researchers. They used transient and steady-state fluid dynamics, thermal models, structural analysis of chimney, collectors (taking into consideration the capability of using ground natural heat storage) in addition to the turbine setup. The following survey conveys some of these studies. The first known attempt to solve Navier-Stokes and Energy Equations for the natural laminar convection in steady-state, predicting its thermo-hydrodynamic behaviour using CFD (Computational Fluid Dynamics) for convective flow in an SCPP was conducted by Bernardes, et al [4]. The employed approach was the "Finite Volumes Method" in generalized coordinates allowing for detailed visualization of the effects of geometrical and operational characteristics. A mathematical model describing fluid flow and heat

transfer has been set up for the three regions of the solar chimney power plant: collector, chimney and turbine. was conducted by Rabehi, R., Chaker, A., Ming, T., & Gong, T [5]. The Spanish prototype was chosen as an example for numerical simulation the results revealed that the variation of solar radiation has an evident effect on the flow and heat transfer characteristics. Meanwhile, the influence of turbine pressure drop on the collector efficiency was slight, while has a considerable effect on the power output. Based on the data from the prototype of Manzanares, Padki, and Sherif [6] elaborated extrapolated SCPP models for medium-to-large scale power generation. Yan, et al [7] described a more comprehensive analytical model for SCPP by using practical engineering correlations obtaining equations for air velocity, airflow rate, power output, and thermo-fluid efficiency. Kroger and Buys [8] developed analytical relations for determining the pressure differential due to frictional effects and heat transfer correlations for developing radial flow between the roof and the collector. Pasumarthi and Sherif [9] built an SCPP small-scale demonstration prototype to study the effect of various geometric parameters on the air temperature, air velocity, and power output of the solar chimney. Further studies were conducted by Pasumarthi and Sherif [10] to exploit the collector performance by extending the collector base and by introducing an intermediate absorber. According to them, both enhancements helped to increase the overall chimney power output. In addition, a brief economic assessment of the system costs was presented.

The objective of this paper is to develop a model that simulates the behaviours of the solar chimney system and study the effect of the chimney height on the performance of the solar chimney power plant with and without thermal storage.

2 Mathematical Model

The basic operation principles behind solar chimney are summarized as follows:

1- Heat is received by the solar collector due to solar irradiation from the sun.

2- Air is heated in the solar collector mostly by convection from the absorber.

3- Hot air is then moving into the chimney due to the buoyancy and stack effect induced in the system. The three components of the solar chimney system; collector, chimney, and turbine are simulated, and the mathematical model is presented below.

2.1 Assumptions

1. One-dimensional heat transfers through the system layers in the (z-direction).
2. There is no heat transfer in the direction of the flow, the energy transferred in the flow direction by mass transfer.
3. The heat losses from the collector edges are negligible.
4. Properties of the cover, absorber, and insulation are independent of temperature variation (constant).
5. The sky can be considered as a black body for long-wavelength radiation at an equivalent sky temperature
6. Dust and dirt on the collector are negligible.
7. Y metric Axis flow of the air inside the collector ($\partial/\partial\theta=0$)
8. The main direction of flow in the collector is in (r) direction, no flow in z, and θ directions. ($u_z = u_\theta = 0$)

9. For the flow through the collector passage and at each (r), the pressure is constant in the vertical direction. $\frac{\partial p}{\partial z} = 0$

10. The collector is over a plane surface.

11. Constant height of collector cover, i.e. radial inward flow is considered between two parallel plates.

12. The heat losses through the walls of the chimney are neglected; and the flowing humid air is considered as a mixture of two ideal gases.

13. The upwind flow is due to the buoyancy force only.

14. The flow in the collector considered a laminar flow.

Under the above assumptions, the continuity equation for each segment of the collector becomes:

$$(\rho u_r A)_{r+dr} = (\rho u_r A)_r \, , m_{r+dr}^{\cdot} = m_r^{\cdot}$$

where:

$$\dot{m}_{coll} = \dot{m}_{chim} \qquad (1)$$

$$\dot{m}_{chim} = \rho_{chim} * V_{chim} * A_{chim} \qquad (2)$$

$\dot{m}_{coll}$: Air mass flow rate through the collector.

ρ_{chim}: Density of air through the chimney.

V_{chim}: Velocity of air through the chimney.

A_{chim}: Cross-sectional area of the chimney.

2.2 Solar Collector Analysis

In the mathematical model, the solar chimney collector is considered as a control volume contains a number of radial sections each section consists of four nodes in different media (cover, air gap, absorber, ground, or insulator underneath of the absorber). The nodes are distributed in a perpendicular plane to the airflow direction as indicated in Figures (1).
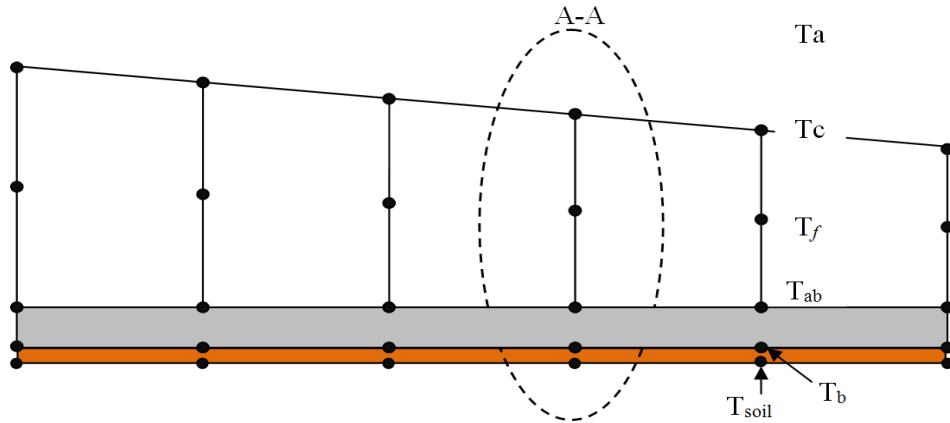
Figure 1: Discretization of solar collector.

2.2.1 Thermal Analysis of the Solar Collector

The useful energy output Q_u of the collector of area A_{coll} is the difference between the absorbed solar radiation and the thermal energy loss. Therefore:

$$Qu = A_{Coll}\left[S_I - U_t\left(T_C - T_{amb}\right) - U_b\left(T_{ab} - T_{Soil}\right)\right] \qquad (3)$$

Where S_1 is the intensity of solar radiation that absorbed by the absorber layer, U_t is the top loss coefficient (W/m^2 K), U_b is the back loss coefficient (W/m^2 K), T_c is the cover temperature, T_{amb} is the outside air temperature, T_{ab} is the absorber temperature and T_{soil} is the soil temperature under the absorber. The thermal efficiency η_{cool}, which is defined as the ratio of the net useful energy collected by collector (Q_u) to the total incident solar radiation and expressed by the Hottel-Whillier-Bliss equation [11] as.

$$\eta_{coll} = \frac{Q_u}{Q_{in}}$$

$$Q_{in} = I \times A_{coll} \qquad (4)$$

where, (I) is the intensity of solar radiation (W/m$^{2)}$, A_{coll} is the collector surface area (m^2), and Q_{in} is the amount of solar radiation received by the collector at its cover.

As is shown in Figure (2), a part of solar radiation I, is reflected to the sky, another part is absorbed by the cover and the rest is transmitted through the cover to the absorber as short-wave radiation. The percentage of the solar rays transmitted through the transparent cover of the collector is called the transmissivity of the cover ((τ_c)$_c$) and the percentage being absorbed by the cover is called the absorptivity of the cover α_c (α_c). Thus, the intensity of solar radiation that absorbed by the absorber layer can be expressed as:

$$S_I = I \times (\tau_c)_{c \times \alpha_{ab}} (5)$$

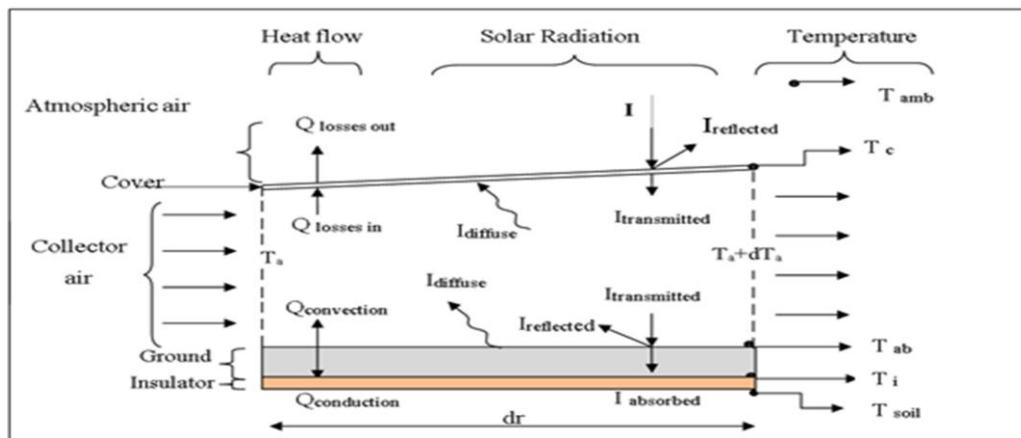where α_{ab}: the absorptivity of the absorber.

Figure 2: Control volume of the solar collector.

As the collector absorber absorbs heat, its temperature is getting higher than that of the surrounding, therefore some amount of the heat transfers to the air inside the collector by convection and to the cover by radiation, also some of the heat is lost by conduction to the ground

underneath the absorber. The rest of energy is stored inside the absorber. The rate of heat loss (Q_{out}) depends on the collector overall heat transfer coefficients (U_t, U_b) and the temperature differences.

$$Q_{out} = \{U_t\,(T_c - T_{amb}) + U_b\,(T_{ab} - T_{Soil})\} \times A_{coll} \quad (6)$$

Where Ut is the top overall heat losses coefficient (W/m^2 K) and Ub is the back overall heat losses coefficient (W/m^2 K). From Figure (1), the energy balance for each subdivision of the collector such as the section in details (A-A) could be presented as a thermal network.

2.2.1.1 The Cover

The thickness of the cover is very thin, then it reasonable to consider a uniform temperature through it. Therefore, a negligible heat storage within the cover could be assumed. The energy balance at a cover differential volume of thickness (δc) and area of (2πr dr) can be presented as:

$$\left[h_w(T_{amb} - T_c) + h_{c-a}(T_a - T_c) + h_{r_{ab-c}}(T_{ab} - T_c) + h_{r_{c-s}}(T_s - T_c) + S_2 \right] = 0 \quad (7)$$

where: $S_2 = I\,\alpha_c$ and $h_w = 5.7 + 3.8\,V_w$

h_w is the convection heat transfer coefficient between the cover and the ambient (W/m^2 K) and V_w is the wind velocity (m/s). h_{c-a}: Convection heat transfer coefficient between the cover and the air in the collector (W/m^2 K).

$h_{r\ ab-c}$: Radiation heat transfer coefficient between the absorber and the cover (W/m^2 K).

$h_{r\ c-s}$: Radiation heat transfer coefficient between the cover and the sky.

Rearranging (7) can be written as:

$$T_c = \frac{\left(h_w T_{amb} + h_{c-a} T_a + h_{r_{ab-c}} T_{ab} + h_{r_{c-s}} T_s + I\alpha_c \right)}{\left(h_w + h_{c-a} + h_{r_{ab-c}} + h_{r_{c-s}} \right)} \quad (8)$$

2.2.1.2 The air between the cover and the absorber

Consider a control volume on the air gap inside the solar collector. The heat balance of the air passage through the control volume can be written as:

$$[h_{c-a}(T_c - T_a) + h_{ab-a}(T_{ab} - T_a)](2\,\pi\,r\,dr) = dQ_u \qquad (9)$$

The mean temperature at each section is calculated as:

$$T_a = \frac{T_{a_{out}} + T_{a_{in}}}{2} \qquad (10)$$

where:

$T_{a_{in}}$, $T_{a_{out}}$, T_a inlet, outlet, and average air temperatures at the collector sections[K],

The useful heat transferred to the moving air stream can be written in terms of the mean fluid and inlet temperature is,

$$dQ_u = 2\,\dot{m}\,C_p\;(T_a - T_{a_{in}}) \qquad (11)$$

From equations (9) and (11):

$$[h_{c-a}(T_c - T_a) + h_{ab-a}(T_{ab} - T_a)](2\,\pi\,r\,dr) = 2\,\dot{m}\,C_p\;(T_a - T_{a_{in}}) \qquad (12)$$

T_a can be calculated from equation (12) as:

$$T_a = \frac{\left(h_{c-a}T_c + h_{ab-a}T_{ab} + \frac{\dot{m}\,C_p}{\pi\,r\,dr}T_{a_{in}}\right)}{\left(h_{c-a} + h_{ab-a} + \frac{\dot{m}\,C_p}{\pi\,r\,dr}\right)} \qquad (13)$$

2.2.1.3 The absorber

As the absorber of collector absorbs heat, its temperature will rise and becomes higher than that of the surrounding, therefore some amount of heat transfers to the air inside the collector by convection and some of heat transferees by radiation to the cover, also some of the heat is lost by conduction to the ground underneath the absorber. The rest of energy is stored inside the absorber. Assuming the absorber has a uniform temperature throughout the absorber, the energy balance at differential

control volume of the absorber of thickness (δ_{ab}) and area of ($2\pi r\, dr$) can be presented as:

$$h_{ab-a}(T_a - T_{ab}^t) + h_{r_{ab-c}}(T_c - T_{ab}^t) + U_{Gr-ab}(T_{soil} - T_{ab}^t) + S_I = \frac{\delta_{ab} \times \rho_{ab} \times c\left(T_{ab}^{(t+\Delta t)} - T_{ab}^t\right)}{\Delta t} \qquad (14)$$

$$T_{ab}^{t+\Delta t} = T_{ab}^t \left[1 - \frac{(h_{ab-a} + h_{ab-c} + U_{Gr-ab}) \times \Delta t}{\delta_{ab}\,\rho_{ab}\,C}\right] + \left[1 - \frac{(h_{ab-a}T_a + h_{ab-c}T_c + U_{Gr-ab}T_{soil} + S_i) \times \Delta t}{\delta_{ab}\,\rho_{ab}\,C}\right] \qquad (15)$$

where: $S_I = I.\tau_c.\alpha_{ab}$, $U_{Gr-ab} = \dfrac{K_i\ K_{soil}}{\delta_i\,K_{soil} + \delta_{soil}\,K_i}$

T_{ab}: Absorber temperature (K).

T_{soil}: Ground temperature underneath the absorber (K).

δ_{ab}: Absorber thickness (m).

T_{soil}: Soil temperature under insulation layer (K).

U_{Gr-ab}: Over all heat transfer coefficient underneath the absorber (W/m^2. K).

K_{ab}: Thermal conductivity of the absorber (W/m K).

δ_i: Insulator thickness (m).

k_i: Thermal conductivity of the insulator (W/m K).

Superscript (t) is the time at which the absorber temperature is considered.

2.2.1.4 The insulation and the ground underneath the absorber

Considering the conduction heat transfer between the insulation and the absorber and heat loss through insulation to ground, the heat energy balance for the insulation layer can be written as:

$$\frac{K_i}{\delta_i}(T_{ab} - T_i) + \frac{K_{soil}}{\delta_{soil}}(T_{Soil} - T_i) = 0 \qquad (16)$$

Then:

$$T_i = \frac{\left(\frac{K_i}{\delta_i}T_{ab} + \frac{K_{soil}}{\delta_{soil}}T_{Soil}\right)}{\left(\frac{K_i}{\delta_i} + \frac{K_{soil}}{\delta_{soili}}\right)} \qquad (17)$$

Where, T_{Soil} is the soil temperature under insulation layer (K), δ_i is the insulator thickness (m) and K_i is the thermal conductivity of the insulation (W/m K).

Estimating the convection heat transfer coefficients is a very complex process. Therefore, simplified correlations were used for estimating the convection heat coefficients. Table (1,2) shows a sample of these correlations [12,13].

Table 1: Correlations and heat transfer coefficient for a laminar flow, free convection

Free convection $Nu_m = 0.54Ra^{1/4}$ $Nu_m = 0.14Ra^{1/3}$	$10^4 \leq Ra < 10^7$, upper or lower heated horizontal surface, Churchill and Chu (1975) $10^7 \leq Ra \leq 10^{11}$, upper or lower Heated horizontal surface, Churchill and Chu (1975)	
State	$T_C < T_a$	$T_C > T_a$
Heat convection coefficient between cover and air in the collector [12].	$1.32 \left(\dfrac{T_a - T_C}{dr}\right)^{1/4}$	$0.59 * \left(\dfrac{T_a - T_{ab}}{dr^2}\right)^{1/4}$
State	$T_{ab} > T_a$	$T_{ab} < T_a$
Heat convection coefficient of absorber and air in the collector [12].	$1.32 \left(\dfrac{T_{ab} - T_a}{dr}\right)^{1/4}$	$0.59 * \left(\dfrac{T_a - T_{ab}}{dr^2}\right)^{1/4}$

Where: dr is the collector section length in the flow direction (m) and Superscript (c) denotes the cover.

Table 2: Correlations for forced (flat plate, constant temperature) [13]

Equations	Flow regime/source
Forced convection $$Nu_m = \frac{1}{\sqrt{\pi}}\sqrt{Rex} \; \frac{Pr}{(1+\; 1.7Pr^{1/4}+21.36\,Pr)^{1/6}}$$	Laminar, $Re < 5 \; x10^5$, Baehr and Stephan (1996)
$$Nu_{m,lam} = 2\,Nu_x$$ $$Nu_m = \frac{0.037Re^{0.8}\,Pr}{1+2.443Re^{-0.1}\;(Pr^{\;2/3}-1)}$$	$5x10^5 < \; Re \; < 10^7, \; 0.6 < \; Pr < 2000$ Petukhov and Popov (1963)
$$Nu_m = \sqrt{Nu_{m,lam}^2 + Nu_{m,tur}^2}$$	Schlichting et al. (1999)

To determine the radiation heat transfer coefficients, the conventional relation is used as:

$$h_{r_{ab-c}} = \frac{\sigma(T_{ab}^2+T_c^2)(T_{ab}+T_c)}{1/\varepsilon_{ab}+1/\varepsilon_c-1} \tag{18}$$

The radiative heat transfer coefficient between the cover (c) and sky (s) is given as:

$$h_{r_{c-s}} = \frac{\sigma\varepsilon_c(T_c^2+T_s^2)(T_c+T_s)(T_c-T_s)}{(T_c+T_{amb})} \tag{19}$$

The atmosphere temperature is given by Swinbank (1963) (Duffie and Backman [14]):

$$T_s = 0\,0552 * T_{amb}^{1.5} \tag{20}$$

Where: T_{amb} is the ambient temperature (K).

The chimney analysis

The chimney converts the heat flow $\dot{Q}$ produced by the collector into kinetic energy and potential energy. Thus, the density difference of the air is caused by temperature difference in the collector works as

driving force. The pressure difference Δp_{tot} is produced between chimney base and the ambient [15].

$$\Delta p_{tot} = \int_0^{H_{chim}} (\rho_{amb} - \rho_{chim}) g\, \delta H \qquad (21)$$

$$\Delta p_{tot} = (\rho_{chim} - \rho_{amb}) g \cdot H_{chim} \qquad (22a)$$

Also $\quad \rho_{chim} = \dfrac{P_{chim}}{RT_{chim}}\ ,\ \ \rho_{amb} = \dfrac{P_{amb}}{RT_{amb}}\ \ and\ \ P_{chim} \cong P_{amb}$

Then: $\Delta p_{tot} = \rho_{chim} * g * H_{chim} * \dfrac{\Delta T}{T_{amb}} \qquad (22b)$

where: H_{chim}: Chimney height (m).

ρ_{amb}: Air density at ambient temperature (kg/m^3).

ρ_{chim}: Air density through the chimney (kg/m^3)

Thus Δp_{tot} increases with chimney height. The total pressure difference causing the draught in the chimney increases with chimney height and the density difference. Also Δp_{tot} can be divided into a static, dynamic and friction pressure drops [16].

$$\Delta p_{tot} = \Delta p_{st} + \Delta p_d + \Delta p_{friction} \qquad (22)$$

The standard definition for dynamic pressure:

$$\Delta p_d = \frac{1}{2} \rho_{chim} V^2{}_{chim} \qquad (23)$$

Δp_s is the static pressure difference drops at the turbine, when considering the system without the turbine, Then: $\Delta p_{st} \cong 0 \qquad (24)$

Now introducing the pressure drop through the chimney due to friction loss $\Delta p_{friction}$, which is directly proportion at to the kinetic energy per unit volume and chimney height H_{chim} and inversely proportion at to the hydraulic diameter of the chimney, D_{chim}. Then:

$$\Delta p_{friction} = \frac{1}{2} f \frac{H_{chim}}{D_{chim}}\ \rho_{chim} V^2{}_{chim} \qquad (25)$$

Where f, is the proportionality coefficient, the dimensionless "Darcy friction factor" or "flow coefficient" and denoted as (f). From the

above-mentioned equation, the pressure drop due to the friction losses is proportional to the kinetic energy per unit volume by the dimensionless term ($f \frac{H_{chim}}{D_{chim}}$) which can be denoted by (ξ). $\xi = f \frac{H_{chim}}{D_{chim}}$.

Then equation (4-26) can be written as:

$$\Delta p_{friction} = \xi \frac{1}{2} \rho_{chim} V^2_{chim} \tag{26}$$

$$\Delta p_{tot} = \frac{1}{2} \rho_{chim} V^2_{chim} + \xi \frac{1}{2} \rho_{chim} V^2_{chim} \tag{27}$$

$$\Delta p_{tot} = \frac{1}{2}(1 + \xi) \rho_{chim} V^2_{chim} \tag{29a}$$

Using equation (22b) in equation (29a) then,

$$V_{chim} = \sqrt{\frac{2*g*H_{chim}}{(1+\xi)} * \frac{\Delta T}{T_{amb}}} \tag{29b}$$

With the total pressure difference and the volume flow of the air at $\Delta p_{st} = 0$, the power P_{tot} contained in the flow is now:

$$P_{tot} = \Delta p_{tot} * V_{chim} * A_{chim} \tag{30}$$

From which the efficiency of the chimney η_{chim} can be found as [17]:

$$\eta_{chim} = \frac{P_{tot}}{\dot{Q}} \tag{28}$$

Where: $\dot{Q} = \dot{m} c_p (\Delta T)$

Actual subdivision of the pressure difference into a static and a dynamic component depends on the energy with drawn by the turbine. Without turbine, a maximum flow speed of V_{chim} is achieved and the whole pressure difference is used to accelerate the air and is thus converted to kinetic energy [16].

$$P_{tot} = \frac{1}{2}(1 + \xi)\dot{m} V^2_{chim} \tag{29}$$

By substituting Eg (22-b) in to Eg (30) and then in to Eg (31), the chimney efficiency can be written as [20]:

$$\eta_{chim} = \frac{g * H_{chim}}{c_p * T_{amb}} \tag{33}$$

This simplified representation explains one of the basic characteristics of the solar chimney, which is that the chimney efficiency is dependent only on its height.

The total power resulting from the air flow:

$$P_{tot} = \eta_{chim} * Q_u = \frac{g * H_{chim}}{c_p * T_{amb}} * \rho_{chim} * c_p * V_{chim} * \Delta T * A_{chim} \tag{34}$$

$$P_{tot} = \frac{g * H_{chim}}{T_{amb}} * \rho_{chim} * V_{chim} * \Delta T * A_{chim} \tag{35}$$

The turbine Analysis

The heat flow produced by the collector is converted into kinetic energy (convection current) and potential energy (pressure drop) through the chimney. The air density difference is caused by the temperature rise in the collector. The air moves upward and works as a driving force. The lighter column of air in the chimney produced pressure difference Δp_{tot}[18] which is equal to,

$$\Delta p_{tot} = \Delta p_{tur} + \frac{1}{2} \rho_{chim} V^2_{chim} + \xi \frac{1}{2} \rho_{chim} V^2_{chim} \tag{36}$$

If the turbine extracts a fraction (xtm) of the total driving potential Δp_{tot} then [16];

$$\Delta p_{tur} = xtm * \Delta p_{tot}$$

Now equation (36) can be written as:

$$\Delta p_{tot} = xtm * \Delta p_{tot} + \frac{1}{2} \rho_{chim} V^2_{chim} + \xi \frac{1}{2} \rho_{chim} V^2_{chim} \tag{37}$$

The air velocity through the chimney becomes:

$$V_{chim} = \sqrt{\frac{2 * \Delta p_{tot}(1 - xtm)}{\rho_{chim}(1 + \xi)}} \tag{38}$$

Substituting equation (22b) into equation (38) the result is,

$$V_{chim} = \sqrt{2 * g * H_{chim} \frac{\Delta T}{T_{amb}} * \frac{(1-xtm)}{(1+\xi)}} \qquad (39)$$

The turbine theoretical useful power P_{tur} becomes:

$$P_{tur} = V_{chim} * A_{chim} * \Delta p_{tur} \qquad (40)$$

The power of wind turbine takes its maximum value when:

$$\frac{dP_{tur}}{dV} = 0$$

$$\frac{dP_{tur}}{dV} = 0 = \Delta p_{tot} - (1 + \xi) \frac{3}{2} \rho_{chim} V^2{}_{chim} \qquad (41)$$

$$V_{chim} = \sqrt{\frac{2}{3} * \frac{\Delta p_{tot}}{\rho_{chim}(1+\xi)}} \qquad (42)$$

Comparing equation (42) with equation (39), the maximum power can be reached when:

$$xtm = \frac{2}{3}$$

And the volumetric flow rate can be estimated by:

$$\dot{V} = V_{chim} * A_{chim} \qquad (43)$$

Then equation (40) can be written as:

$$P_{tur} = \dot{V} * \Delta p_{tur} \qquad (44)$$

The maximum power is achieved when two thirds of the total pressure difference is utilized by the turbine and can be expressed as:

$$P_{tur,max} = \frac{2}{3} \eta_{coll} * \eta_{chim} * A_{coll} * I \qquad (45)$$

$$P_{tur,max} = \frac{2}{3} * \eta_{coll} * \frac{g}{c_{p} * T_{amb}} * H_{chim} * A_{coll} * I \qquad (46)$$

The maximum electrical power from the solar chimney is obtained by multiplying equation (46) by the turbine efficiency that contains both blade, transmission and generator efficiencies [18].

$$P_{electric} = P_{tur,max} * \eta_{tur} \qquad (47)$$

Numerical solution procedure

The proposed solution method was implemented by utilizing the MATLAB software, which has been built according to the reliable equations discussed previously to evaluate the performance and thermal behaviour of a solar chimney power plant.

The mathematical model was programmed and designed using the GUI technique as shown in Figure (3); this technique allows the user to enter all the specified model variables used in the simulation and also provides easy access to changing these variables without physically changing the program code. Before running the simulation, the user must enter the desired solar tower power plant specifications
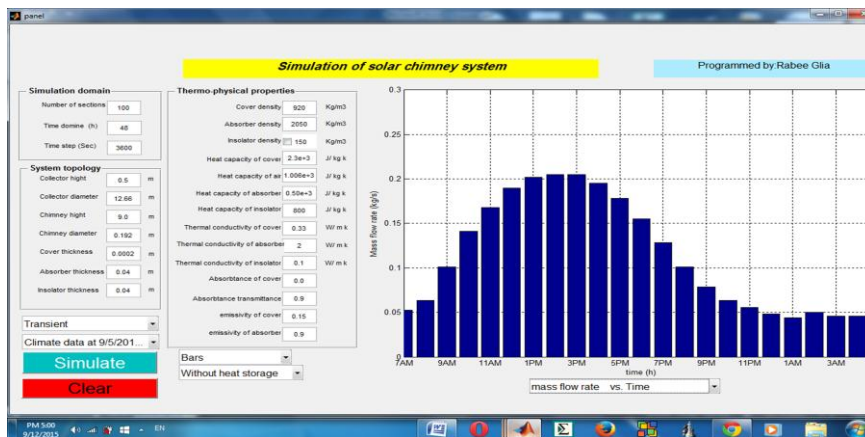

Figure 3: GUI of mathematical model.

Validation of the theoretical model

The solution to the above theoretical model is obtained using a self-developed MATLAB program. The calculated results are compared with the experimental data of the experimental data that were collected from a small pilot solar chimney; The experiment was conducted in the

Faculty of Engineering in Sabratha [19] also with the experimental data of the Spanish prototype to validate the theoretical model.

Comparison between theoretical and experimental results.

Four days with different ambient temperatures and different values of solar radiation are considered for comparison of the behavior of the solar chimney system when it operated with and without water containers as thermal storage. The comparison covered the air velocities through the chimney and temperatures at the entrance of the chimney. The comparison is presented in figures (4 to 5). Figure (4) shows the comparison between mathematical model results and the experimental data when the solar chimney system is not provided by water containers as thermal storage. Figure (5) shows the comparison between mathematical model results and the experimental results when the solar chimney system is provided by water containers as thermal storage. Obviously, there is good agreement between the experimental and theoretical results. It should be noted that the theoretical model used the same climate data that was recorded during the tests.
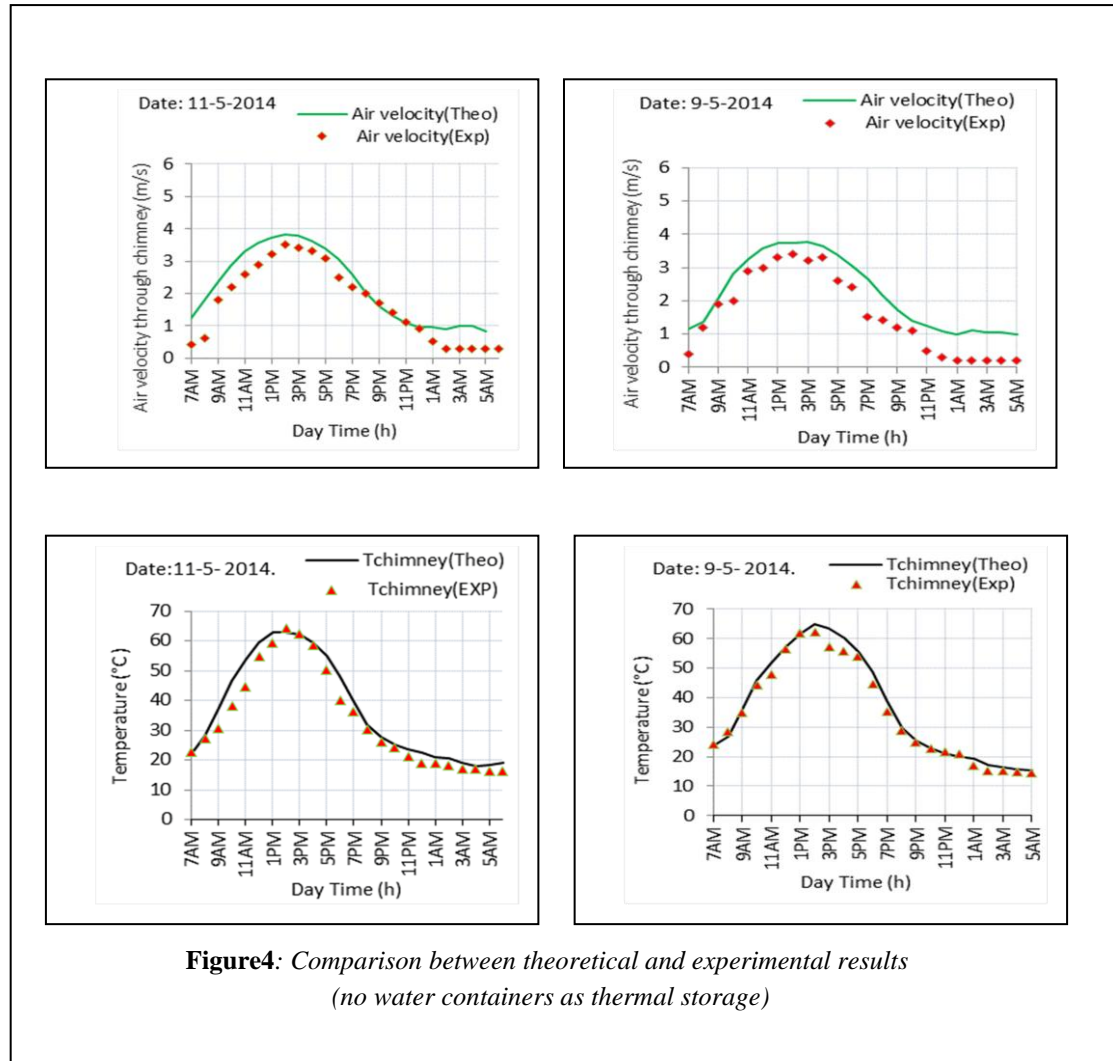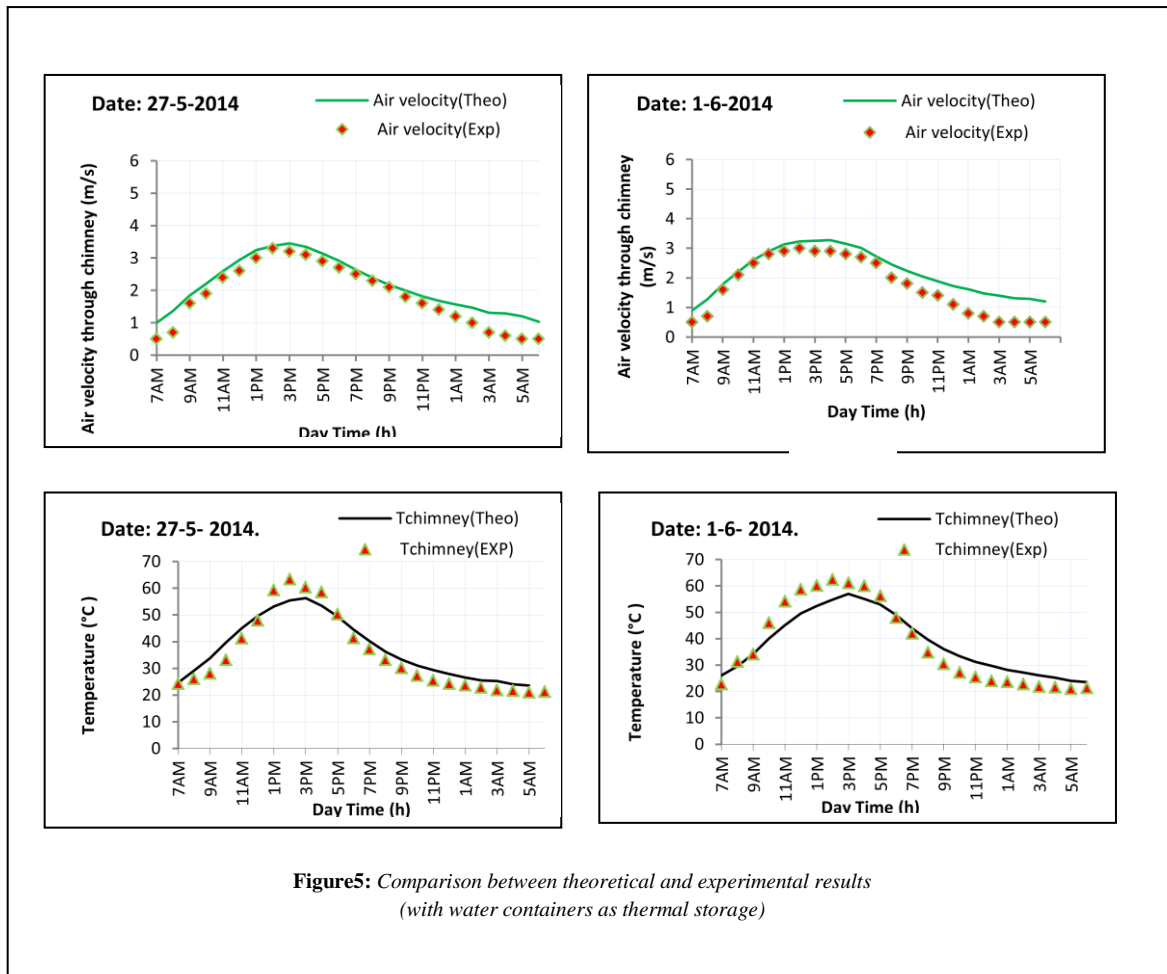
Figure4: *Comparison between theoretical and experimental results
(no water containers as thermal storage)*

Figure5: *Comparison between theoretical and experimental results*
(with water containers as thermal storage)

Validation of the Model results with the experimental result from the prototype solar chimney power plant in Manzanares, Spain.

The solution to the above theoretical model is obtained using a self-developed MATLAB program. The calculated results are compared with the experimental data of the Spanish prototype to validate the theoretical model. The main dimensions of the Spanish prototype are listed in Table 3.

Table 3: The main dimensions and technical data for the prototype solar chimney power plant in Manzanares, Spain [20, 21].

Tower height	194.6 m
Tower radius	5.08 m
Mean collector radius	122.0 m
Mean roof height	1.85 m
Number of turbine blades	4
Turbine blade profile	FX W-151-A
Blade tip speed to air transport velocity ratio	1: 10
Operation modes	stand-alone or grid connected mode
Typical collector air temp. increase	$\Delta T = 20$ K
Nominal output	50 kW
Coll. covered with plastic membrane	40'000 m²
Coll. covered with glass	6'000 m²

The model results are compared with the experimental result from the prototype solar chimney power plant in Manzanares, Spain [20, 21]. Figures (6 to 9) show the air temperatures, velocity, and power output *vs.* solar time. In general, good agreement was obtained between the model results and the published measured data.

In Figure (9) the main operational data, i.e., solar intensity, updraft velocity, and electric power output, are shown for a typical day. It shall be pointed out: that, there is still an updraft during the night, which can be used to generate power during the night.
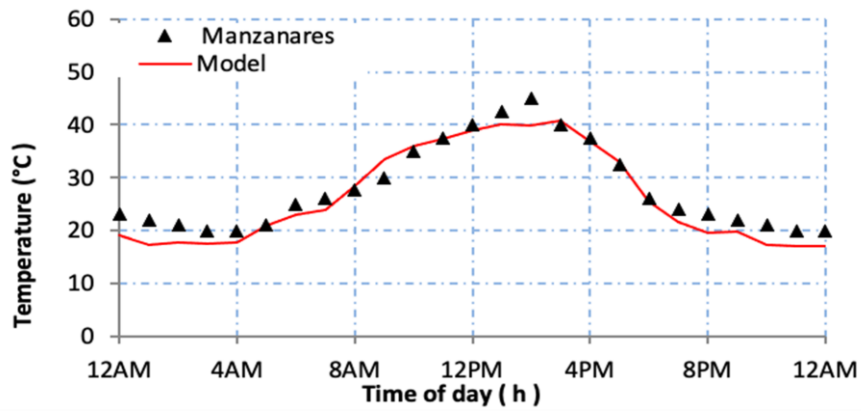
Figure 6: Comparison between model results and measurements from Manzanares [22]: (updraft air temperatures for a typical Day June 18th, 1987)
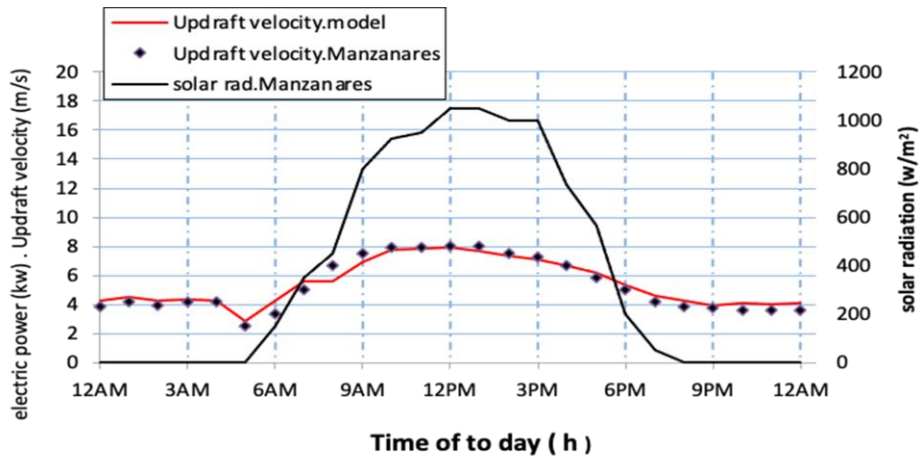

Figure7: Comparison between model results and measurement from Manzanares [23] (updraft velocity for a typical Day June 18th, 1987)

Figure8: Comparison between model results and measurement from Manzanares[23]
(power output for a typical Day June 18th, 1987)

Figure9: *Comparison between model results and measurement from Manzanares [23]*
(updraft velocity and power output for a typical Day June 18th, 1987)
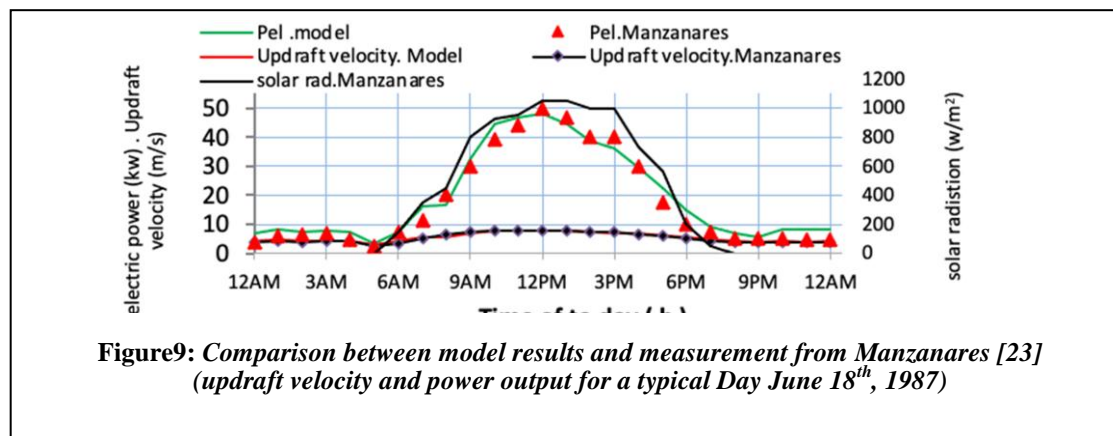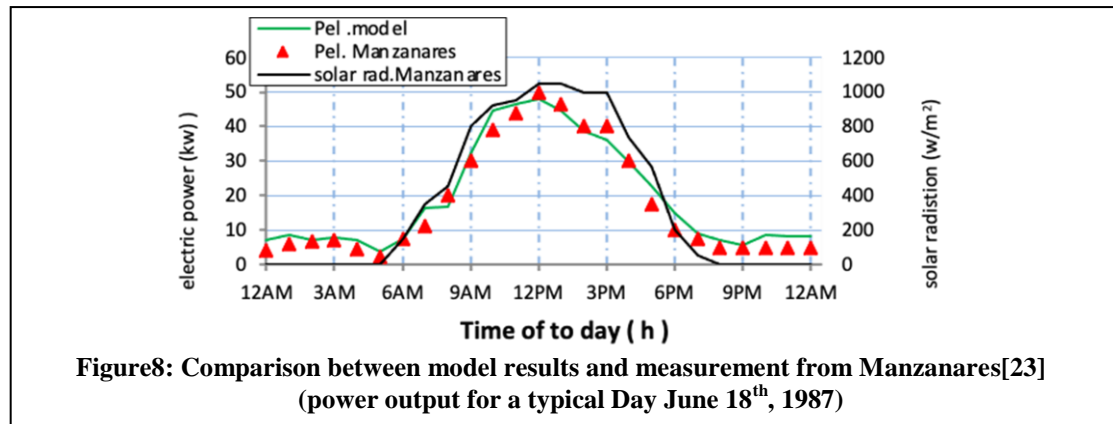
Effect of chimney height on the power output of an SCPP

The dimensions were taken from the prototype solar chimney power plant in Manzanares, Spain. data are shown in Table 3, and the external climatic conditions were taken of temperature, wind speed, and solar radiation were taken from the experimental data that were collected from a small pilot solar chimney; The experiment was conducted in the Faculty of Engineering in Sabratha [19]. That is to study the effect of the chimney height on the solar chimney power plant by constant the dimensions solar collector and change the height of the chimney. For every chimney height, the maximum power output point is selected as the indicator of the power output of the SCPP system. The calculated curve of power output versus the chimney height is shown in Fig. 10. Obviously from the figure, the power output increases with the chimney height

increase، when the solar radiation 857 W/m^2 is selected. According to the tendency shown in Fig. 10 the relationship between energy output and the height of the chimney is positive, but at high chimney heights, the increase in energy output needs to be investigated compared to the cost of building the chimney. Because the highest chimney investigated in the literature is only 1500 m [24] and humans have no experience in constructing gigantic chimney higher than 1000 m till now, the maximum chimney height places no limitation on the chimney height for power output from practical points. Accordingly, there is no need to consider the limitation on chimney height in the design of a large-scale SCPP under current technology.
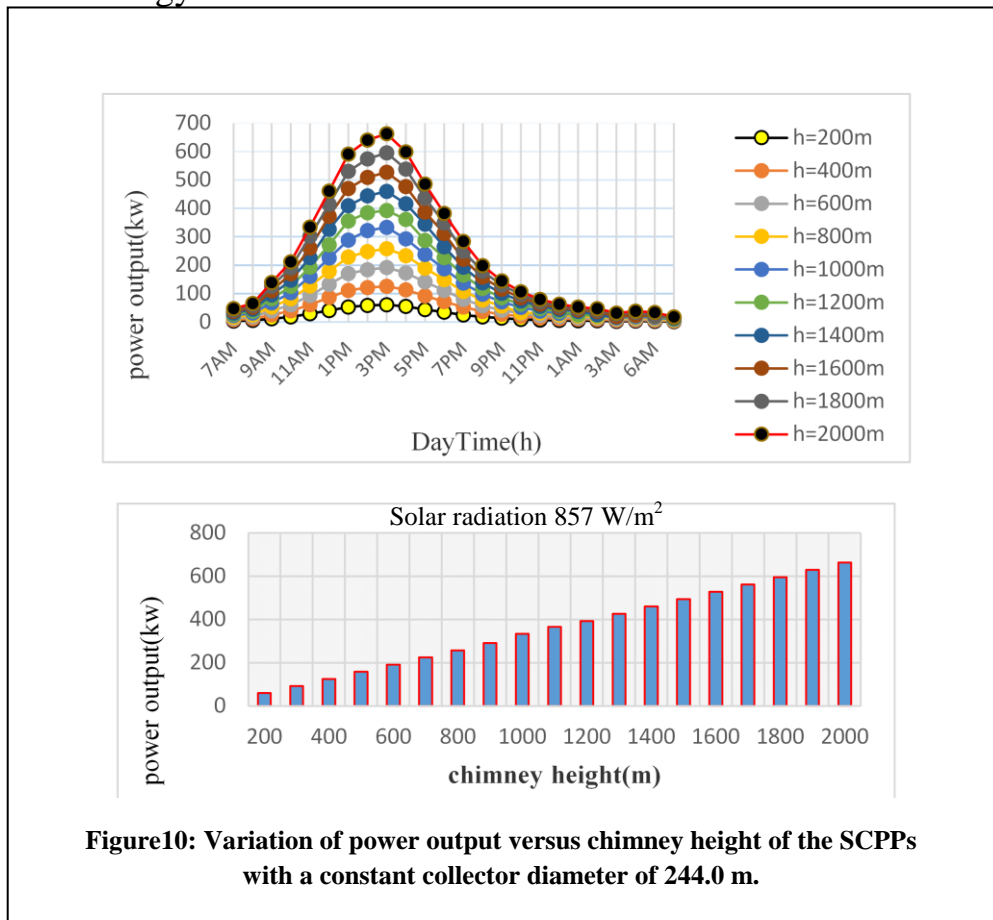

Figure10: Variation of power output versus chimney height of the SCPPs with a constant collector diameter of 244.0 m.

3   Conclusions

This paper presents an analytical model for predicting the performance of a chimney solar power plant. The model showed good agreement with that of the experiment and prototype solar chimney power plant in Manzanares, Spain. However, there are some differences due to assumptions and idealizations of the analysis. Various conclusions can be drawn from the results as follows:

1. Temperature difference between collector air performance and environment can reach high values during the summer in Libya that generates a stream of air that can drive a wind turbine and Generate electricity from the generator. This means that the solar chimney system can be operated to generate electricity in Libya.

2. The floor of the solar collector stores part of the thermal energy. Energy during the day and gives it free for the night; therefore, the use of absorbents is the high thermal capacity of SCPP. It is important to start generating electricity after sunset.

3. As the standard lapse rate of atmospheric temperature is used, the maximum power output of 662.89 kW is obtained for the solar radiation of 857W/m² at the chimney height of 2000m.

4. The higher the chimney height, the higher the energy output. However, this increase should be compared to the cost of building very high chimneys.

Nomenclature

A	Area (m^2)		α	Absorptance.
C	Specific heat (J/kg K)		Δ	Differential.
D	Diameter (m)		ε	The emissivity.

dr	Incremental radius (m)	η	The efficiency.
f	Darcy friction factor	ρ	Density (kg/m^3).
g	Gravitational acceleration (m/s^2)	τ	The transmittance of the cover.
H	Height (m)	ξ	The overall friction coefficient of the chimney.
h	Convection heat transfer coefficient (W/m^2 K)	δ	The thickness (m)
h_r	Radiation heat transfer coefficient (W/m^2 K)	*amb*	Ambient
I	Global horizontal irradiance (W/m^2)	*chim*	Chimney
K	Thermal conductivity (W/mK)	*soil*	Ground under insulation
Nu	Nusselt number	*coll*	Collector
Qi	Rate of energy input (W)	*f*	Friction
Qu	Rate of useful energy output(W)	*tur*	Turbine
r	Radius (m)	*w*	Wind
S_1	Solar radiation absorbed by the absorber (W/m^2)		
S_2	Solar radiation (W/m^2)		
T	Temperature (K &˚C)		
U	Heat losses coefficient (W/m^2 K)		
V	Air velocity through chimney (m/s)		
$\dot{\forall}$	Volumetric flow rate (m^3/s)		
$\dot{m}$	Mass flow rate (kg/s)		
xtm	Turbine pressure extraction factor (Pa)		

4 *References*

[1] Haaf W, Friedrich K, Mayr G, Schlaich J. (1983), Solar chimneys. Part I: Principle and construction of the pilot plant in Manzanares. Into J Solar Energy; 2:3–20.

[2] *Hamdan, M. O., Rabbata, O. (2012), "Experimental solar chimney data with analytical model prediction", World Renewable Energy Forum Denver, CO May 13-17.*

[3] *Ahmed, O. K., & Hussein, A. S. (2018). New design of solar chimney (case study). Case studies in thermal engineering, 11, 105-112.*

[4] *Bernardes, M. A. d. S., et al. (1999), Numerical Analysis of Natural Laminar Convection in a Radial Solar Heater, International Journal of Thermal Sciences, 38, 42-50.*

[5] *Abehi, R., Chaker, A., Ming, T., & Gong, T. (2018). Numerical simulation of solar chimney power plant adopting the fan model. Renewable Energy, 126, 1093-1101.*

[6] *Padki, M. M., and S. A. Sherif (1989), Solar chimney for medium-to-large scale power generation, paper presented at Proceedings of the Manila International Symposium on the Development and Management of Energy Resources, Manila, Philippines.*

[7] *Yan, M. Q., et al. (1991), Thermo-fluid analysis of solar chimneys, paper presented at American Society of Mechanical Engineers, Fluids Engineering Division (Publication) FED, Publ by ASME, Atlanta, GA, USA.*

[8] *Kroger, D. G., and J. D. Buys (1999), Radial Flow Boundary Layer Development Analysis, South African Inst. of Mechanical Eng. R & D J., 15, 95-102.*

[9] *Pasumarthi, N., and S. A. Sherif (1998a), Experimental and theoretical performance of a demonstration solar chimney model - Part I: Mathematical model development, International Journal of Energy Research, 22, 277-288.*

[10] *Pasumarthi, N., and S. A. Sherif (1998b), Experimental and theoretical performance of a demonstration solar chimney model -*

Part II: Experimental and theoretical results and economic analysis, International Journal of Energy Research, 22, 443-461.

[11] DUFLIE, J. A. (1991). Solar engineering of thermal processes. A Wiley-Interscience Publication, 770-781.

[12] Holman, J.P., "Heat Transfer", 10th Edition. McGraw-Hill Company, New York, 1997.

[13] Bernardes, M. A. d. S., et al. (2003), Thermal and Technical Analyses of Solar Chimneys, Solar Energy, 75, 511-524.

[14] Gannon, A. J., and T. W. Von Backstrom (2003), Solar chimney turbine performance, Journal of Solar Energy Engineering, Transactions of the ASME, 125, 101-106.

[15] Schlaich, J., et al. (2003), Design of commercial solar tower systems - Utilization of solar induced convective flows for power generation, paper presented at International Solar Energy Conference, Kohala Coast, HI.

[16] Weinrebe, G., Schiel, W., "Up-Draught Solar Tower and Down-Draught Energy Tower—A Comparison," Proceedings of the ISES Solar World Congress 2001, Adelaide, Australia, 2001.

[17] T. C. Miqdam and A. K. Hussein, ―Basement kind effects on air temperature of a solar chimney in Baghdad-Iraq weather, ‖ International Journal of Applied Sciences, vol.2, n° 2, pp.12-20, 2011.

[18] F. Cao, L. Zhao, H. Li, and L. Guo, ― Performance analysis of conventional and sloped solar chimney power plants in China, ‖ Applied Thermal Engineering, vol. 50, no 1, pp. 582-592, 2013.

[19] Galia, R. A., Arebi, B. H., & Shuia, E. M (2017), Investigation of Solar Chimney System and the Effect of Thermal Storage Capacity on the System Performance Part I: Experimental Investigation.

[20] *Petela, R. (2009), Thermodynamic study of a simplified model of the solar chimney power plant, Solar Energy, 83, 94-107.*

[21] *Zhou, X., et al., Analysis of Chimney Height for Solar Chimney Power Plant, Applied Thermal Engi-neering, 29 (2009), 1, pp. 178-185.*

[22] *Nizetic, S., Ninic, N., Klarin, B., Analysis and Feasibility of Implementing Solar Chimney Power Plants in the Mediterranean Region, 33 (2008), 11, pp. 1680-1690.*

[23] *J. Schlaich, R. Bergermann, W. Schiel, and G. Weinrebe, ―Design of Commercial Solar Updraft Tower Systems—Utilization of Solar Induced Convective Flows for Power Generation, ‖ Journal of Solar Energy Engineering, vol. 127, no 1, p. 117, 2005.*

[24] *Gannon AJ, von Backström TW. Solar chimney cycle analysis with system loss and solar collector performance. Journal of Solar Energy Engineering e Transactions of the ASME 2000; 122(3):133e7.*